Title
Handheld electromagnet carrier for transfer of hyperpolarized carbon-13 samples

Journal
Magnetic Resonance in Medicine, 75(2)

ISSN
0740-3194

Authors
Shang, Hong
Skloss, Timothy
von Morze, Cornelius
et al.

Publication Date
2016-02-01

DOI
10.1002/mrm.25657

Peer reviewed

HHS Public Access

Author manuscript

Magn Reson Med. Author manuscript; available in PMC 2017 February 01.

Published in final edited form as:

Magn Reson Med. 2016 February ; 75(2): 917–922. doi:10.1002/mrm.25657.

Hand-held Electromagnet Carrier for Transfer of Hyperpolarized Carbon-13 Samples

Hong Shang[1,2], **Timothy Skloss**[3], **Cornelius von Morze**[1], **Lucas Carvajal**[1], **Mark Van Criekinge**[1], **Eugene Milshteyn**[1,2], **Peder E.Z. Larson**[1,2], **Ralph E. Hurd**[3], and **Daniel B. Vigneron**[1,2]

[1]Department of Radiology and Biomedical Imaging, University of California, San Francisco, San Francisco, California, USA

[2]UCSF - UC Berkeley Graduate Program in Bioengineering, San Francisco / Berkeley, California, USA

[3]GE Healthcare, USA

Abstract

Purpose—Hyperpolarization of ^{13}C nuclei by dissolution Dynamic Nuclear Polarization (DNP) increases SNR by >10,000 fold for metabolic imaging, but care must be taken when transferring hyperpolarized (HP) samples from polarizer to MR scanner. Some ^{13}C substrates relax rapidly in low ambient magnetic fields. A hand-held electromagnet carrier was designed and constructed to preserve polarization by maintaining a sufficient field during sample transfer.

Methods—The device was constructed with a solenoidal electromagnet, powered by a non-magnetic battery, holding the HP sample during transfer. A specially designed switch automates deactivation of the field once transfer is complete. Phantom and rat experiments were performed to compare MR signal enhancement with or without the device for HP [^{13}C]urea and [1-^{13}C]pyruvate.

Results—The magnetic field generated by this device was tested to be > 50 Gauss over a 6 cm central section. In phantom and rat experiments, [^{13}C]urea transported via the device showed SNR improvement by a factor of 1.8–1.9 over samples transferred through the background field.

Conclusion—A device was designed and built to provide a suitably high yet safe magnetic field to preserve hyperpolarization during sample transfer. Comparative testing demonstrated SNR improvements of approximately 2-fold for [^{13}C]urea while maintaining SNR for [1-^{13}C]pyruvate.

Keywords

Hyperpolarized carbon-13 MRI/MRSI; dynamic nuclear polarization; low magnetic field; T1 relaxation; scalar coupling; urea

Correspondence to: Daniel B. Vigneron, 1700 4th Street, Byers Hall Suite 102F, MC 2512, San Francisco, CA 94158-2330, TEL: (415) 476-3343, Dan.Vigneron@ucsf.edu.

Submitted for the 22th Annual Meeting of the ISMRM, Milan, Italy 2014

Introduction

Hyperpolarized (HP) Carbon-13 MRI with dissolution Dynamic Nuclear Polarization (DNP) (1) has recently been shown to provide biologic information on previously inaccessible aspects of metabolic processes by detecting endogenous, nontoxic ^{13}C-labeled probes to monitor enzymatic conversions through key biochemical pathways (2–4). Since both spatial and chemical information are encoded, this new molecular imaging modality allows simultaneous detection of multiple biologic compounds and metabolic products with sensitivity enhancements of >10,000 fold (1). The recently completed Phase 1 clinical trial conducted at UCSF demonstrated the safety and feasibility of HP ^{13}C-pyruvate MRI in prostate cancer patients without any dose-limiting or other notable toxicities (5).

Some HP ^{13}C substrates can lose polarization extremely quickly in low magnetic field when they are transferred between the polarizer and the MR scanner, reducing the SNR. For example, scalar coupling between fast-relaxing quadrupolar ^{14}N and ^{13}C results in rapid loss of polarization of [^{13}C]urea (6). Although most *in vivo* HP ^{13}C MRI studies have focused on probing metabolism using metabolically active substrates (7), several studies have shown that metabolically inactive agents like [^{13}C]urea can be applied to angiography or perfusion imaging (8, 9). HP [^{13}C]urea for perfusion MRI has advantages over conventional gadolinium(Gd)–containing (paramagnetic) contrast agents including direct proportionality of signal to concentration, inherently high contrast-to-noise ratio (CNR) due to the absence of background signal, and an excellent safety profile potentially benefitting studies in patients currently excluded from contrast imaging studies. Also, [^{13}C]urea can be co-polarized with [1-^{13}C]pyruvate for combined perfusion and metabolic imaging (10, 11). Urea is a safe, endogenous compound with normally high concentrations *in vivo* (typically 1–10 mM, and much higher in the renal medullary interstitium), low toxicity, and neutral pH, as well as the key MR properties of long T_1 relaxation time and high polarization by DNP. Recent studies have also demonstrated the ability of HP [^{13}C]urea to investigate changes in urea transport and concentration in the kidney (12).

In previous studies, this loss of polarization of [^{13}C]urea during sample transfer has been addressed by carrying a permanent magnet next to the HP sample, or at the molecular level by secondary labeling with ^{15}N (6, 13). However, the cost of [^{13}C,$^{15}N_2$]urea is about 5 times higher than [^{13}C]urea. Furthermore, J-coupling in [^{13}C,$^{15}N_2$]urea splits the ^{13}C NMR resonance peak into a triplet thus lowering the signal amplitude and potentially confounding quantitation. The permanent magnet method raises safety concerns since it could fly into the scanner causing harm. In addition, permanent magnets provide non-uniform fields and are especially impractical for large samples. To address these limitations, we constructed and tested a new electromagnet carrier device to provide a suitable and relatively uniform magnetic field for the safe transfer of HP samples for ^{13}C MR studies.

Theory

Spin-lattice relaxation depends on several independent mechanisms, including interactions with paramagnetic centers and scalar coupling between fast-relaxing quadrupolar nuclei, which cause faster relaxation when the magnetic field decreases. Quadrupolar nuclei with

spin > 1/2 (e.g. ^{14}N) have very short T_1. The scalar coupling of ^{13}C to ^{14}N provides a relaxation mechanism for ^{13}C as ^{14}N is undergoing very rapid T_1 relaxation. The scalar coupling relaxation rate can be calculated by Eq. 1.

$$R_{sc}=\frac{8\pi^2 J^2}{3} I(I+1)\frac{T_1}{1+(\Delta\omega)^2 T_1^2} \quad [1]$$

In Eq. 1, R_{sc} is the scalar coupling relaxation rate, J is the scalar coupling constant in Hz, I is the spin quantum number of the coupled nucleus (I_{14N}=1), T_1 is the spin-lattice relaxation time of the quadrupolar nucleus (^{14}N), $\Delta\omega=\omega_{13c}-\omega_{14N}$ is the difference in Larmor frequencies of coupled nuclei ^{13}C and ^{14}N. For this mechanism to be very effective, the Larmor frequencies of these two nuclei must be very close. This condition is met at low magnetic fields such as during HP sample transfer, although it may also occur at high field, for example for ^{13}C (15.087 MHz) and ^{79}Br (15.023 MHz) at 1.41T (14). One approach to reduce the scalar coupling relaxation mechanism is to increase the external magnetic field.

Methods

Simulation & Background Field Measurements

The ambient magnetic field through which the HP samples were transferred was measured with a three-axis Hall effect magnetometer (model THM 7025, Metrolab Technology SA, Switzerland), as shown in Figure 1A. The distance of 0m corresponds to the location of the DNP polarizer, while the distance of 15.4m corresponds to the center of the MR scanner. R_{sc} can be estimated as a function of magnetic field based on Eq.1, given parameters measured in (6), including T_1=1.0±0.1ms, J=14.5±0.1Hz, as shown in Figure 1B. Assuming a piece-wise constant relaxation rate along the path and constant transfer velocity over a 6s transfer, the signal decay curve can be estimated along this path, as plotted in Figure 1C.

By adding a magnetic field offset of 50 G (along vertical direction) in simulation, this scalar coupling relaxation mechanism can be significantly reduced as shown in Figure 1B, resulting in a 1.83-fold signal improvement at the end of the path, as shown in Figure 1C. This field strength specification was used for the design of this device in order to provide an adequate magnetic field to maintain a long T_1 for HP samples during transfer.

Hardware

The electromagnet carrier device was designed to provide a suitable magnetic field for the safe transfer of HP samples. The key part of the device is a solenoid with a current of 0.5A powered by a non-magnetic battery to generate a relatively uniform magnetic field of >50 G over a 6 cm longitudinal section. The size of the solenoid was customized for the specific 3mL and 5mL syringes (BD, Franklin Lakes, NJ) commonly used for preclinical HP ^{13}C studies. The inner diameter was designed to be 1.65 cm and the length 7.9cm. The gauge of the wire (22 AWG) and number of layers (6 layers) were chosen based on the desired field of 50 G, resulting in a total of 727 turns.

The circuit is shown in Figure 2A. A single-cell (3.7V) 500mAH lithium-ion polymer (LiPo) battery (E-flite/Horizon Hobby, Champaign, Illinois) composed of non-magnetic materials powered the magnetic field. The device can be safely carried into the 3T MRI scanner room and turned off there. The current was activated by depressing the default-open, pushbutton momentary switch. When the button was released the current was turned off automatically. The design of the switch ensures that the device can be safely operated in the scanner room, covering the entire sample transfer path and thus minimizing the loss of polarization. A LED was installed to indicate when the device is activated. The battery can provide stable current for at least 1 hour of continuous use. The sample transfer duration is < 10s, so one battery charge can last for hundreds of HP experiments.

The device (in Figure 2C) was constructed using a combination of custom 3D printed parts and commercially available parts meeting the design criteria for performance, non-magnetic materials, and durability. The housing was built with strength to withstand drops to the floor and the shape was designed for ease of carrying and standing upright. The switch was trigger-mounted to enable easy depression, holding and releasing of the button. The battery was attached on the surface of the device in a manner allowing easy replacement or charging. The inner diameter of the solenoid-encompassed sample chamber closely fits the syringes, which are quickly guided through a conical opening on top of the coil, as shown in figure 2B.

Magnetic Field Measurements

The strength, stability, and uniformity of the device magnetic field were simulated and measured. The magnetic field strength along the central axis was first simulated based on the Biot-Savart Law. Assuming that the magnetic field in the solenoid is uniform so that the field strength along the central axis approximates the field inside the solenoid. The same magnetometer described above was used to measure the field inside the solenoid. The solenoid for the actual device had a smaller inner diameter, which was customized for the sample size. This smaller size was too narrow for the probe of the magnetometer. Therefore a prototype solenoid with larger size was constructed in order to test the accuracy of the field simulation by comparisons with the measured results.

HP MR Phantom Experiments

Experiments were performed to test the effect of the device on HP [^{13}C]urea and copolarization of [^{13}C]urea and [1-^{13}C]pyruvate. Dissolution DNP was performed with a HyperSense polarizer (Oxford Instruments, Oxford, UK) operating at 1.3 K and 3.35 T, using previously described methods, generating 4.5mL 100mM HP media (11). MR experiments were performed on a 3T clinical MRI scanner (GE Healthcare, Waukesha, WI, USA) with a broadband RF amplifier. Custom built, dual-tuned mouse birdcage coils (l=8cm, d=5cm) were used for RF transmission and signal reception. The RF transmit gain was calibrated with a ^{13}C enriched urea phantom with similar size and similar location as HP phantom.

After dissolution, the HP sample was divided into two equally apportioned syringes, and both were carried to the scanner at the same speed along the same path. One was transferred

in the ambient field, while the other was transferred with this device. The device was turned on during DNP dissolution and kept activated throughout the transfer from DNP polarizer to MR scanner. It was deactivated at around 2m away from the center of MR scanner where the fringe field is already sufficiently large. The device was held vertically during transfer such that the magnetic field from this device was added to the fringe field instead of potentially cancelling each other. The sample transfer took approximately 6s.

The solutions were then injected into two fixed syringe reservoirs already lying inside the coil, oriented along the longitudinal direction. The signal of these two samples was then acquired together with one pulse sequence and approximately the same local B_0 and B_1 fields. In this manner, the differences in signal between the samples transferred with and without the device were calculated from the same experiment, while controlling for any variations in initial polarization, total amount of sample, and transfer duration. Another control group experiment was done with the same imaging methods, but both samples were transferred without the device. The urea-only experiment and control group experiment were repeated four times respectively, and the copolarization experiment was repeated five times.

For the urea-only tests, the axial images were acquired with single shot EPI readout, with no localization along the longitudinal direction. The acquisitions used a flip angle=90°, TE=100ms, TR=250ms, matrix size=20×20, FOV=10×10cm. For urea and pyruvate copolarization tests, a dynamic 1D MRSI sequence was used with hard pulse excitation (0.5ms duration), double spin echo refocusing and symmetric EPI readout (15). Spatial encoding was only applied along the×direction (right/left) with projections along y and z directions. Localization along this direction enabled separation of the samples transferred with and without the device. The readout gradient duration was 100ms giving a spectral resolution of 10Hz, with spectral bandwidth of 543 Hz to include the resonances of both pyruvate and urea. For image reconstruction, the even and odd EPI lobe data were combined by the sum-of-squares method. The data were acquired using a flip angle=10°, TE=140ms, and TR=2s. Although the amounts of HP material in each syringe were approximately equal, the signal at thermal equilibrium was also measured to compensate for any potential residual differences in the amount of HP sample in each syringe.

HP MR in vivo Experiments

HP [^{13}C]urea *in vivo* rat experiments were performed using a balanced SSFP sequence (13) to acquire a coronal image (projection along A/P direction) following an IACUC-approved protocol. The experiments were repeated twice on the same animal, one with HP sample transferred in ambient field, the other transferred with this device, while keeping all the other parameters the same. [^{13}C]urea was polarized for 88±1 min and transferred to the scanner within 7s. 2.5mL 100mM solution was injected into a rat through tail vein catheter over 12s with image acquisition starting at 20s after the beginning of injection. The imaging parameters were: flip angle=60°, TR=15ms, matrix size=140×70, FOV=20×10cm, sequential phase encoding.

Results

Magnetic Field Tests

The simulated and measured magnetic field distributions within the solenoid are shown in Figure 3. Figure 3A corresponds to the larger prototype solenoid, while Figure 3B corresponds to the actual solenoid used in this device. The measured results were close to the simulated results, but slightly higher in the center, as shown in Figure 3A. Using the same simulation method, we calculated the magnetic field of the device to be > 50 G over a 6 cm central section, as shown in Figure 3B. Even though the magnetic field drops quickly at both ends, the field is relatively uniform in the 3cm central section where HP media is usually placed. When holding the switch and keeping the electric current on for about 30 seconds (sample transfer usually takes less than 10s), the measured magnetic field remained constant, thereby demonstrating the stability of the device.

HP MR Tests

In the HP [^{13}C]urea phantom experiments, the [^{13}C]urea signal in both syringes is shown in one axial image (e.g. Figure 4A). The SNR increase achieved by using this device was demonstrated by the ratio of image intensity. The results showed a significantly ($p = 0.012$) higher (1.9±0.2) [^{13}C]urea signal using the device. The result of the control group demonstrated a small effect between syringe locations (+4%). However, this effect was much smaller than the experimental signal ratio (~1.9), and therefore does not alter the conclusion that SNR increased by about 2-fold. Also, this small effect in the control group failed to reach statistical significance ($p = 0.098$).

For the HP copolarization phantom experiments, spectroscopic imaging was acquired to distinguish the different compounds based on frequency, and the different samples transferred with and without the device based on spatial location. The spectra were analyzed for each resonance and each transfer approach (e.g. Figure 4B). The data showed a significantly ($p = 0.002$) higher (1.9±0.3) [^{13}C]urea signal intensity in the sample transferred with the device. [1-^{13}C]pyruvate signal intensity is slightly higher (1.1±0.1), however, it failed to reach statistical significance ($p=0.550$).

The results of HP [^{13}C]urea *in vivo* experiment are shown in Figure 5, along with the corresponding image from a 3D balanced SSFP ^{1}H scan. The coronal ^{13}C image with sample transferred with the device has improved SNR. Quantitatively measuring the SNR at the center of right kidney shows a SNR improvement of 1.8-fold with this device.

Discussion

This device enabled a nearly 1.9-fold SNR improvement of HP urea signal as compared to samples carried in the ambient field, in HP [^{13}C]urea experiments, HP urea and pyruvate copolarization experiments, and one *in vivo* experiment. The observed 1.8–1.9 fold SNR improvement from experiments is close to the expected 1.83-fold increase predicted by simulation, which indicates that the hypothesis of fast signal decay due to scalar coupling relaxation is correct and the model we use (eq.1) is accurate. Therefore this model can be

used for further study with other HP molecules. The SNR improvement may be even more significant in cases where the ambient field along transfer path is lower than in our facility.

Although [1-^{13}C]pyruvate is not affected by scalar coupling relaxation, other relaxation mechanisms could affect it at low field, such as relaxation via paramagnetic centers (radical and gadolinium in solution). However, in our copolarization experiments the [1-^{13}C]pyruvate signal was not significantly different with or without the device. Theoretically the effect of relaxation via paramagnetic centers is small due to very low concentration of radical or gadolinium in the liquid state(16, 17). Furthermore, this possible mechanism would likely have a small effect considering the transfer time is just 6s, as a small fraction of expected T1 value (18). However, use of this device would prevent pyruvate relaxation effects that could occur at very low fields at some locations.

While the initial testing was focused on HP [^{13}C]urea and [1-^{13}C]pyruvate, it could also benefit other compounds. For example, HP [5-^{13}C]glutamine is being developed as a noninvasive imaging marker for glutaminolysis, allowing improved diagnosis and monitoring of glutamine-dependent tumors (19–21). Similar to urea, this substrate is also affected by coupling between ^{13}C and ^{14}N.

Conclusions

A electromagnet carrier device was designed and built to supply a suitable and safe magnetic field (> 50 G) to preserve polarization during HP sample transfer, especially for compounds with scalar coupling between fast-relaxing quadrupolar ^{14}N and ^{13}C, such as in HP [^{13}C]urea. In comparative testing, this device demonstrated SNR improvements of approximately 2-fold for [^{13}C]urea while maintaining the signal of HP [1-^{13}C]pyruvate.

Acknowledgements

The authors acknowledge Jeremy Bancroft Brown for assistance with 3D printing, and Hsin-Yu Chen, Zihan Zhu for assistance with experiments. This work was supported by the UCSF Hyperpolarized MRI Technology Resource Center NIH P41 EB013598, NIH R01 EB013427, NIH K01 DK099451, and GE Healthcare.

References

1. Ardenkjær-Larsen JH, Fridlund B, Gram A, Hansson G, Hansson L, Lerche MH, Servin R, Thaning M, Golman K. Increase in signal-to-noise ratio of >10,000 times in liquid-state NMR. Proc Natl Acad Sci USA. 2003; 100(18):10158–10163. [PubMed: 12930897]
2. Golman K, Ardenkjær-Larsen JH, Petersson JS, Månsson S, Leunbach I. Molecular imaging with endogenous substances. Proc Natl Acad Sci USA. 2003; 100(18):10435–10439. [PubMed: 12930896]
3. Golman K, Thaning M. Real-time metabolic imaging. Proc Natl Acad Sci USA. 2006; 103(30): 11270–11275. [PubMed: 16837573]
4. Chen AP, Albers MJ, Cunningham CH, Kohler SJ, Yen YF, Hurd RE, Tropp J, Bok R, Pauly JM, Nelson SJ, Kurhanewicz J, Vigneron DB. Hyperpolarized C-13 spectroscopic imaging of the TRAMP mouse at 3T-initial experience. Magn Reson Med. 2007; 58(6):1099–1106. [PubMed: 17969006]
5. Nelson SJ, Kurhanewicz J, Vigneron DB, Larson PEZ, Harzstark AL, Ferrone M, van Criekinge M, Chang JW, Bok R, Park I, Reed G, Carvajal L, Small EJ, Munster P, Weinberg VK, Ardenkjaer-Larsen JH, Chen AP, Hurd RE, Odegardstuen L-I, Robb FJ, Tropp J, Murray JA. Metabolic

imaging of patients with prostate cancer using hyperpolarized [1-^{13}C] pyruvate. Sci Transl Med. 2013

6. Chiavazza E, Kubala E, Gringeri CV, Düwel S, Durst M, Schulte RF, Menzel MI. Earth's magnetic field enabled scalar coupling relaxation of ^{13}C nuclei bound to fast-relaxing quadrupolar ^{14}N in amide groups. J Magn Reson. 2013; 227:35–38. [PubMed: 23262330]
7. Kurhanewicz J, Vigneron DB, Brindle K, Chekmenev EY, Comment A, Cunningham CH, DeBerardinis RJ, Green GG, Leach MO, Rajan SS. Analysis of cancer metabolism by imaging hyperpolarized nuclei: prospects for translation to clinical research. Neoplasia. 2011; 13(2):81–97. [PubMed: 21403835]
8. Johansson E, Månsson S, Wirestam R, Svensson J, Petersson J, Golman K, Ståhlberg F. Cerebral perfusion assessment by bolus tracking using hyperpolarized ^{13}C. Magn Reson Med. 2004; 51(3): 464–472. [PubMed: 15004786]
9. Svensson J, Månsson S, Johansson E, Petersson JS, Olsson LE. Hyperpolarized ^{13}C MR angiography using trueFISP. Magn Reson Med. 2003; 50(2):256–262. [PubMed: 12876701]
10. Wilson DM, Keshari KR, Larson PEZ, Chen AP, Hu S, Criekinge MV, Bok R, Nelson SJ, Macdonald JM, Vigneron DB. Multi-compound polarization by DNP allows simultaneous assessment of multiple enzymatic activities *in vivo*. J Magn Reson. 2010; 205(1):141–147. [PubMed: 20478721]
11. von Morze C, Larson PEZ, Hu S, Yoshihara HA, Bok RA, Goga A, Ardenkjaer-Larsen JH, Vigneron DB. Investigating tumor perfusion and metabolism using multiple hyperpolarized ^{13}C compounds: HP001, pyruvate and urea. Magn Reson Imaging. 2012; 30(3):305–311. [PubMed: 22169407]
12. von Morze C, Bok RA, Sands JM, Kurhanewicz J, Vigneron DB. Monitoring urea transport in rat kidney in vivo using hyperpolarized ^{13}C magnetic resonance imaging. Am. J. Physiol. Renal Physiol. 2012; 302(12):F1658–F1662. [PubMed: 22492940]
13. Reed GD, von Morze C, Bok R, Koelsch BL, Van Criekinge M, Smith KJ, Shang H, Larson PEZ, Kurhanewicz J, Vigneron DB. High Resolution C-13 MRI With Hyperpolarized Urea: in vivo T2 Mapping and N-15 Labeling Effects. IEEE T Med Imaging. 2014; 33:362–371.
14. Lyerla JR Jr, Grant DM, Bertrand RD. Field-dependent contributions to carbon-13 nuclear relaxation. J.Phys. Chem. 1971; 75(26):3967–3971.
15. Cunningham CH, Chen AP, Albers MJ, Kurhanewicz J, Hurd RE, Yen Y-F, Pauly JM, Nelson SJ, Vigneron DB. Double spin-echo sequence for rapid spectroscopic imaging of hyperpolarized ^{13}C. J Magn Reson. 2007; 187(2):357–362. [PubMed: 17562376]
16. Caravan P, Ellison JJ, McMurry TJ, Lauffer RB. Gadolinium(III) chelates as MRI contrast agents: Structure, dynamics, and applications. Chem Rev. 1999; 99:2293–2352. [PubMed: 11749483]
17. Gordon JW, Fain SB, Rowland IJ. Effect of lanthanide ions on dynamic nuclear polarization enhancement and liquid-state T1 relaxation. Magn Reson Med. 2012; 68:1949–1954. [PubMed: 22367680]
18. Chattergoon N, Martinez-Santiesteban F, Handler WB, Ardenkjaer-Larsen JH, Scholl TJ. Field dependence of T1 for hyperpolarized [1-^{13}C]pyruvate. Contrast Media Mol. Imaging. 2013; 8(1): 57–62. [PubMed: 23109393]
19. Gallagher FA, Kettunen MI, Day SE, Lerche M, Brindle KM. ^{13}C MR spectroscopy measurements of glutaminase activity in human hepatocellular carcinoma cells using hyperpolarized ^{13}C -labeled glutamine. Magn Reson Med. 2008; 60(2):253–257. [PubMed: 18666104]
20. Keshari KR, Wilson DM. Chemistry and biochemistry of ^{13}C hyperpolarized magnetic resonance using dynamic nuclear polarization. Chem. Soc. Rev. 2014; 43(5):1627–1659. [PubMed: 24363044]
21. Daye, D.; Wellen, KE. Metabolic reprogramming in cancer: unraveling the role of glutamine in tumorigenesis. Elsevier; 2012. p. 362-369.

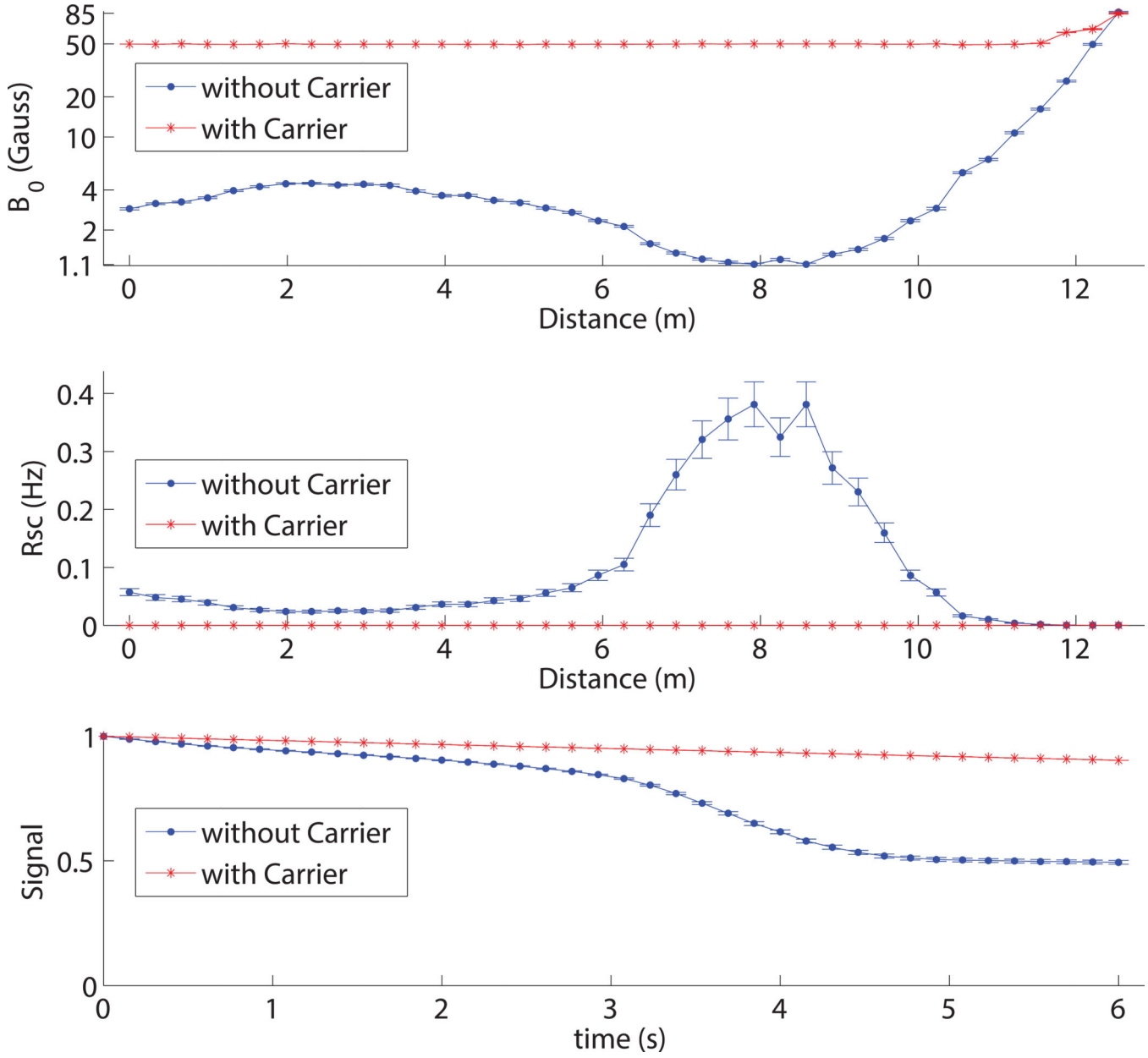

Figure 1.

Measured ambient magnetic field magnitudes along sample transfer path (without carrier, blue line with dots) and simulated field magnitude with 50G added along vertical direction (with carrier, red line with stars) (A). Y axis (B_0) is displayed with a log scale. The distance of 15.4m corresponds to the center of the MR scanner and 0m corresponds to the location of the DNP polarizer. The range of distance (0 m to 13.4 m) corresponds to the part of sample transfer path where the device was used. Estimated scalar coupling relaxation rate of HP [^{13}C]urea along the path corresponding to the two different fields (B). Estimated signal decay curve along the path assuming piece-wise constant relaxation rate and constant transfer speed within 6s (C).

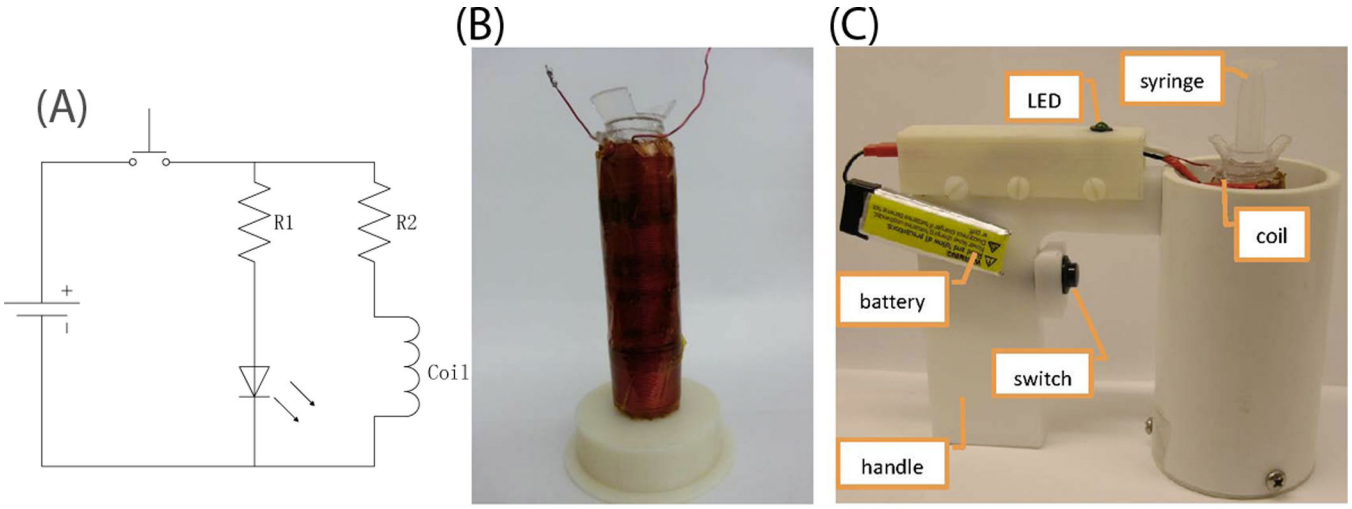

Figure 2.

Hardware design of electromagnet carrier device. Circuit diagram (A). Resistance of coil = 2.9 Ohm, R1 = 833 Ohm, R2 = 4.4 Ohm. A non-magnetic LiPo 500 mAH battery supplies 3.7V and a current of 0.5A in the coil (current in the LED 2.1mA). The switch is a default-open pushbutton momentary switch. Photo of the solenoid inside (B) and photo of the whole device (C).

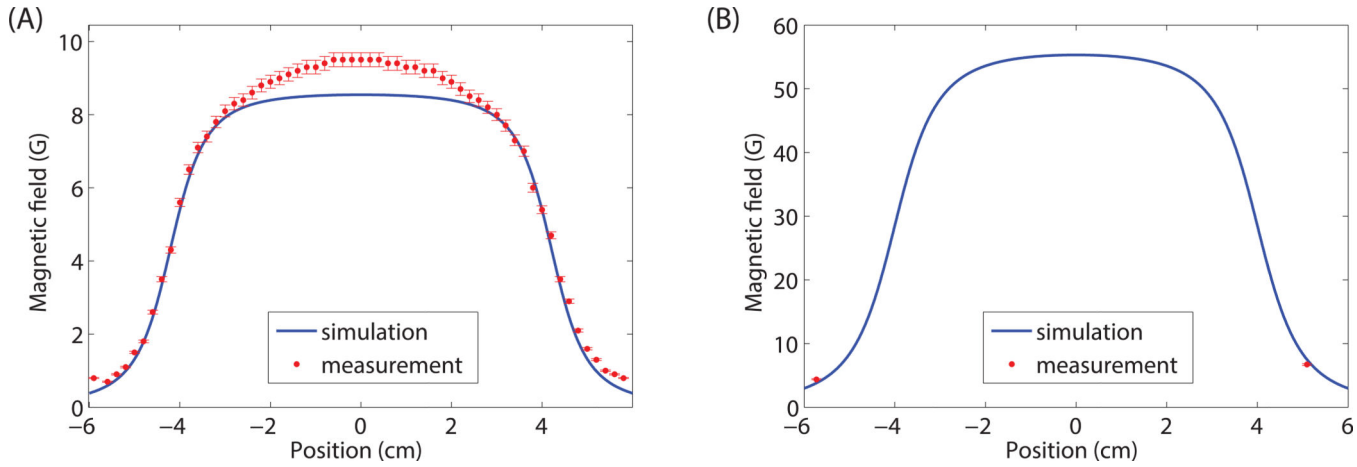

Figure 3.

Simulated (blue line) and measured (red dots) magnetic field distribution in the prototype solenoid with larger diameter (A) and the solenoid used in the device (B). Error of measurement (shown as red error bars) were determined from the accuracy of the magnetometer. The measured field distribution was not available for the solenoid in the device because its size is smaller than the probe of the magnetometer, but the calculation demonstrated a field of greater than 50G over the central 6 cm.

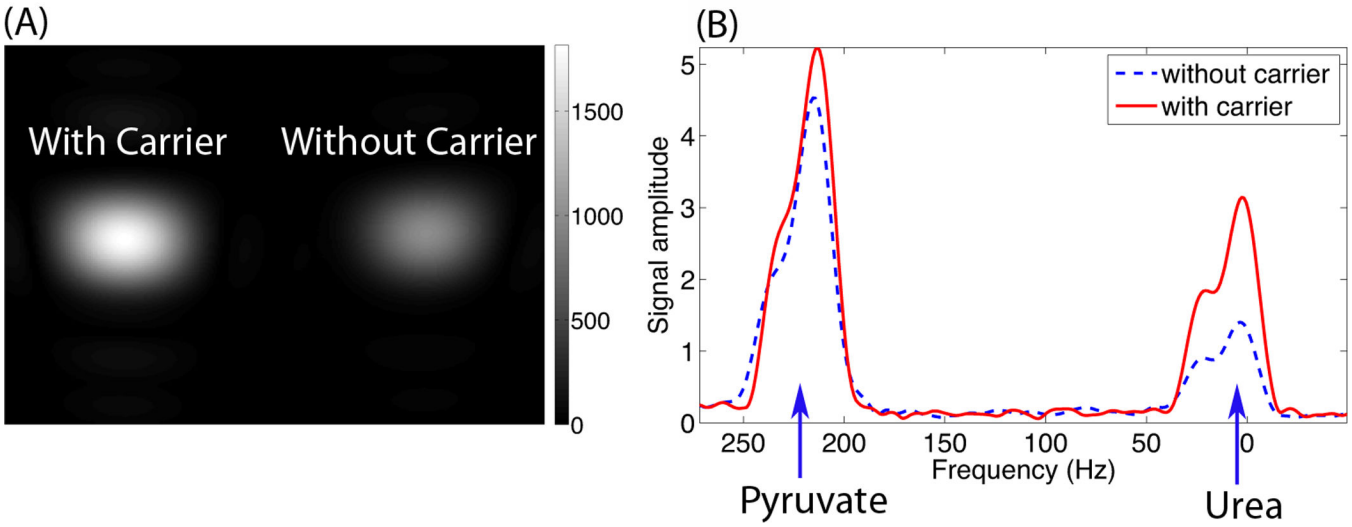

Figure 4.

Example of experimental comparisons between two HP samples scanned in one acquisition, one sample carried with this device (with Carrier), the other carried in ambient field (without Carrier). The just urea experiment was performed using axial ^{13}C MRI (A), while the copolarization of urea and pyruvate MRSI experiment resulted in two spectral peaks corresponding to the two HP compounds acquired from the samples transported with (solid red line) and without the carrier device (dotted blue line) (B). For copolarization results, the left peak corresponds to pyruvate and the right peak corresponds to urea. The center frequency was set close to the urea frequency.

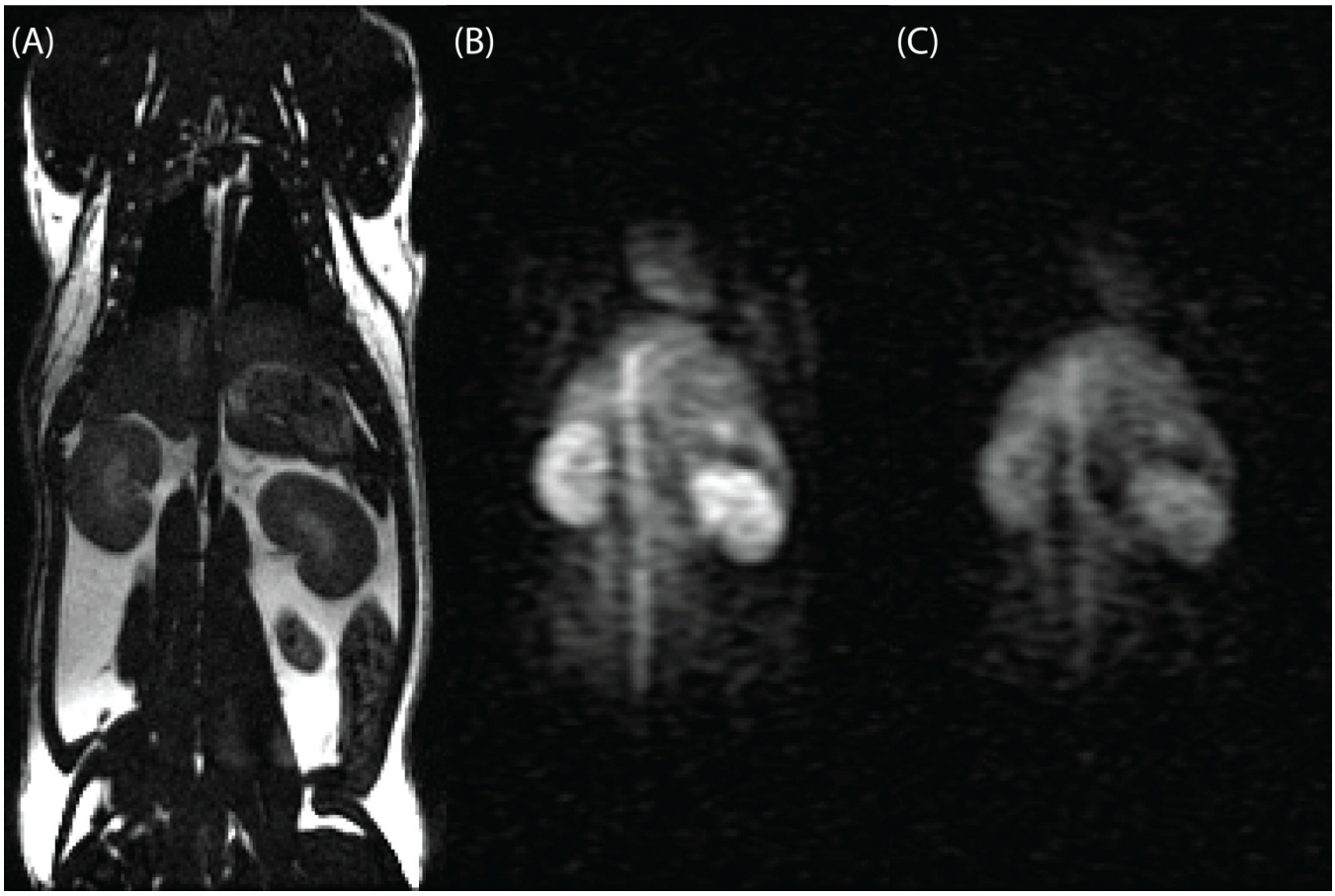

Figure 5.

In vivo rat experiment results. (A) A coronal slice of a ^{1}H 3D balanced SSFP sequence. (B) HP [^{13}C]urea images using a 2D (coronal) balanced SSFP sequence (projection along A/P direction) with sample transferred with this device. (C) The same acquisition repeated on the same animal and position, but with sample transferred in ambient field. (B) and (C) were acquired with the same image parameters and experimental setup and differed only in the transfer method. (B) and (C) are displayed with the same window. SNR (measured at right kidney center) in (B) was 1.8 times higher using this device than without (C).